# 2D Materials in Ultrafast Lasers

Subjects: Nanoscience & Nanotechnology
Contributor: Bo Fu

Ultrafast lasers are the key component of ultrafast photonics, which have come into practice in various fields, such as micromachining, communication, medical procedures, gas detection, and remote sensing. With the advantages of stability, compactness, and easy implementation, mode-locking and Q-switching are two notable techniques to achieve ultrafast pulsed lasers, where SAs perform crucial roles in many types of ultrafast lasers, such as fiber, solid-state, and waveguide lasers.

Keywords: two-dimensional materials ; fabrications ; saturable absorbers ; ultrafast lasers

## 1. Graphene

As the pioneer of 2D materials, graphene came to the first use as SA in 1.5-μm region owing to the telecommunication boom. In 2009, Hasan et al. first reported on an ultrafast laser mode-locked by a solution-processed graphene-polymer at 1557 nm with a pulse duration of ~800 fs [1]. Almost at the same time, Bao et al. demonstrated the use of graphene SA as mode-locker in an erbium-doped fiber laser (EDFL) at 1565 nm, in which a graphene film was synthesized by CVD and coated on the core of a fiber [2]. Subsequently, Zhang et al. employed a graphene-polymer and atomic layer graphene as SAs in an EDFL to achieve large-energy mode-locked pulses with single pulse energies of 3 and 7.3 nJ, respectively [3].

Since this pioneering work, the applications of 2D materials including graphene in ultrafast lasers started flourishing [4]. In 2010, Sun et al. proposed a broadband tunable ultrafast laser mode-locked by graphene at the central wavelengths ranging from 1525 to 1559 nm with a pulse width about 1 ps near transform limitation [5]. Such wavelength-tunable pulsed lasers enjoy great potential in various applications, such as spectroscopy and sensing [6]. **Figure 1**a shows the transmission electron microscope (TEM) image of the folded graphene flake. The output spectra, corresponding autocorrelation traces, and output pulse train are shown in **Figures 1**b–d, respectively.

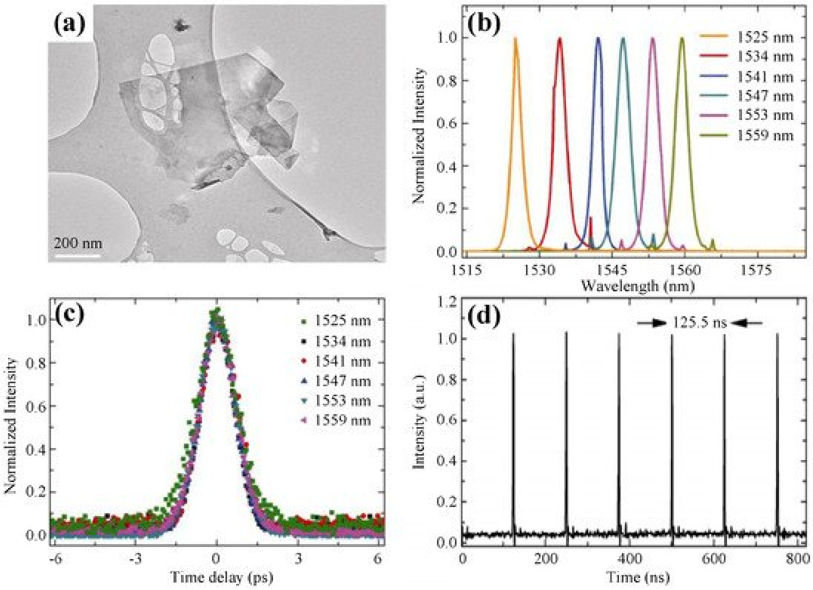


**Figure 1.** The experimental results of mode-locked EDFL enabled by graphene SA. (**a**) TEM image of a folded graphene flake. (**b**) Output spectra. (**c**) Autocorrelation traces. (**d**) Output pulse train. (**a**–**d**) adaped from [5].

After abundant work on mode-locked lasers, graphene started to be applied in Q-switched lasers to gain pulses with high pulse energy [7]. Luo et al. first exploited graphene as SA to obtain Q-switched pulses in EDFL, which achieved dual-wavelength pulses at 1566.17 and 1566.35 nm with a pulse width of 3.7 μs and pulse energy up to 16.7 nJ [8]. In the next year, a graphene-based Q-switched fiber laser with a tunable broadband between 1522 and 1555 nm was demonstrated by Popa et al., in which a pulse width of 2 μm and pulse energy of 40 nJ were obtained [9]. Such a broadband laser could be applied as the light source for metrology [10], biomedical diagnostics [11], and environmental sensing [12].

In 2012, Gao et al. reported on the first use of graphene SA in a Q-switched Er-doped yttrium aluminum garnet (Er:YAG) laser at 1645 nm with a repetition rate of 35.6 kHz and maximum output power of 251 mW [13]. Soon after that, Sobon et al. realized a passive harmonic mode-locked EDFL with atomic multilayer graphene SA, where a high repetition rate of 2.22 GHz was achieved at the 21st harmonic [14]. In 2013, Fu et al. also reported on a 32nd harmonic mode-locked laser with excellent stability, in which the supermode suppression was up to 50 dB and the signal-to-noise ratio (SNR) was better than 67 dB [15]. Cafiso et al. deployed monolayer graphene in a Chromium-doped YAG (Cr:YAG) laser, obtaining stable mode-locked pulses with a short pulse duration of 91 fs [16].

In 2015, Sotor et al. integrated a CVD-grown graphene-polymer composite (60-layer) into a dispersion-managed fiber laser and obtained a stretched mode-locked pulse of 88 fs in 1.5 μm [17]. The study also validated that the modulation depth of multilayer graphene was proportional to the number of its layers, which can reach up to the 10% level. In 2019, Fu et al. demonstrated the bound states of solitons and harmonic mode-locking from a fiber laser based on graphene [18]. The laser could produce 26th harmonic stable pulses with a pulse duration of 720 fs and an SNR of 65 dB at the repetition rate of 409.6 MHz, which promoted the applications of graphene-based lasers, including spectroscopy and nonlinear imaging.

The research of graphene-based ultrafast laser in 1 μm was carried out simultaneously along with that in 1.5 μm. In 2010, Yu et al. reported on the first Q-switched ultrafast laser by employing graphene epitaxially grown on silicon carbide (SiC) in a neodymium-doped YAG (Nd:YAG) crystal laser centered at 1064 nm, obtaining a maximum pulse energy of 159.2 nJ [19]. Subsequently, Zhao et al. proposed the first mode-locked ytterbium-doped fiber laser (YDFL) based on CVD-grown graphene film with a dissipative soliton pulse of 580 ps [20]. In 2011, a graphene-based Q-switched YDFL was demonstrated by Liu et al. [21]. In the experiment, the graphene polyvinyl-alcohol (PVA) composite was deposited on a broadband reflective mirror, and the laser generated stable pulses with a pulse width of 70 ns at maximum output power of 12 mW.

In 2011, Cho et al. proposed the first graphene-based solid-state laser with a tunable wavelength from 1.22 to 1.25 μm, where stable 94-fs pulses with an SNR of 62.2 dB were achieved at a repetition rate of 75 MHz [22]. In 2014, Zhao et al. realized a rectangular pulsed fiber laser mode-locked by microfiber-based graphene, the operating wavelength of which could be set to 1061.8 and 1068.8 nm by tuning the bandpass filter or rotating the polarization controllers [23].

In 2011, Wang et al. first used graphene as SA in a Q-switched thulium-doped YAG (Tm:YAG) laser at the wavelength of 2-μm, achieving a pulse energy up to 1.74 μJ and a maximum average output power of 38 mW [24]. In 2012, Ma et al. reported on the first mode-locked laser enabled by graphene-polymer composite at 2018 nm with a pulse width of 729 fs, where Tm-doped calcium lithium niobium gallium garnet (Tm:CLNGG) crystal was used as gain media [25]. Later, Zhang et al. reported on a Tm-doped fiber laser (TDFL) mode-locked by graphene-polymer, achieving low-noise pulses with a pulse width of 3.6 ps and an SNR of ∼70 dB [26].

Liu et al. achieved the first Q-switched operation based on graphene SA in 2 μm, which possessed a pulse duration of 1.4 μs and a single pulse energy of 85 nJ [27]. These works laid the foundation for the applications of graphene SA in 2-μm region. In 2013, Fu et al. achieved a pulse energy up to 35 nJ in a graphene-based mode-locked Tm-Ho co-doped fiber laser (THDFL), which possessed a tunable waveband from 1897.69 to 1930.27 nm [28]. Jiang et al. proposed an ultrafast TDFL Q-switched by CVD-grown graphene SA with a maximum output power of 96 mW at the repetition rate of 202 kHz [29].

In 2014, Zhao et al. achieved Q-switched pulses in a graphene-based holmium-doped YAG (Ho:YAG) ceramic laser, obtaining a pulse energy up to 9.3 μJ [30]. Furthermore, Fu et al. employed graphene as SA in ytterbium (Yb)-, Er-, and Tm-Ho co-doped fiber lasers successively and all achieved passively mode-locking, which demonstrated the broadband operation property of graphene in wide operating wavelengths from 1 to 2 μm [31].

As for the mid-IR region, the first graphene mode-locked Cr:Zinc Selenide (Cr:ZnSe) laser centered around 2.5 μm was proposed by Cizmeciyan et al. in 2013 [32]. Soon after that, Tokita et al. reported on the first graphene Q-switched laser in 3 μm by incorporating a graphene SA mirror in an Er-doped ZBLAN fiber laser, obtaining a repetition rate of 59 kHz, a pulse width of 400 ns, and an average output power of 380 mW, respectively [33].

In 2015, Zhu et al. demonstrated a mode-locked fiber laser in 3-μm region for the first time based on graphene SA mirror [34]. According to the results, mode-locked pulses had a pulse width of 42 ps at a repetition rate of 25.4 MHz. Without stopping, the working wavelength of ultrafast mode-locked laser based on graphene kept extending, which reached up to 4.4 μm under Pushkin et al.'s work in 2020 [35].

Unfortunately, the application of graphene SA is limited due to its low absorption co-efficiency (2.3% per layer) and absence of bandgap [2][36]. However, the modulation depth of graphene increases with number of its layers, which enables the remarkable performance of graphene in broadband operations [2][37]. Additionally, other merits compared with traditional SA, such as the ultrafast recovery time, lower saturation intensity, and wavelength-independent saturable absorption, make graphene an outstanding SA that is widely used in mode-locked and Q-switched lasers [20][38]. It is the applications of graphene in ultrafast lasers that opened the curtain on the research of 2D materials in ultrafast photonics with excellent performance.

## 2. Topological Insulators

Due to the similarity to graphene in band structure [39][40][41], TIs, such as $Bi_2Te_3$, $Bi_2Se_3$, and $Sb_2Te_3$, have also been widely studied and applied in ultrafast photonics. In 2012, Bernard et al. made a preliminary exploration of the optical properties about $Bi_2Te_3$ and used it as SA to realize a mode-locked fiber laser in the 1.5-μm region [42]. Triggered by this work, Zhao et al. also demonstrated a mode-locked laser based on $Bi_2Te_3$ that was fabricated by the hydrothermal intercalation/exfoliation method [40].

**Figure 2**c,d shows the spectrum centered at 1558.4 nm and the pulse width of 1.86 ps. Scanning electron microscopy (SEM) and TEM images of the as-prepared $Bi_2Te_3$ are shown in **Figure 2**a,b. Later, the saturable absorption property of $Bi_2Se_3$ was experimentally investigated by Zhao et al. from a mode-locked fiber laser with a tunable waveband ranging from 1557 to 1565 nm [39]. This pioneering work paved the path for applications of TIs in ultrafast photonics.

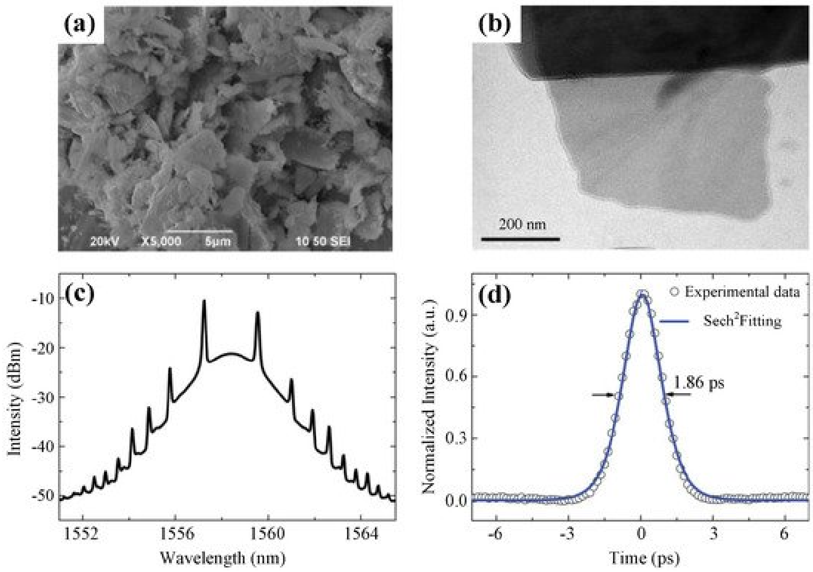


**Figure 2.** The experimental results of mode-locked EDFL enabled by $Bi_2Te_3$ SA. (**a**) SEM and (**b**) TEM images of $Bi_2Te_3$ nanosheets prepared by the hydrothermal intercalation/exfoliation method. (**c**) Soliton spectrum. (**d**) Autocorrelation trace. (**a**–**d**) adapted with permission from [40]. Copyright 2012 American Institute of Physics.

In 2013, Tang et al. obtained Q-switched operation from a $Bi_2Te_3$-induced Er:YAG ceramic laser at 1.645 μm with a maximum output power of 210 mW, which indicated that TIs SAs could be suitable candidates for high-power applications [43]. In the same year, Chen et al. achieved a dual-wavelength fiber laser at 1545.85 and 1565.84 nm, and a wavelength-tunable fiber laser ranging from 1510.9 to 1589.1 nm both Q-switched by $Bi_2Se_3$ successively, which confirmed the potential of TIs in broadband optical operation [44].

In 2014, Lee et al. demonstrated a femtosecond mode-locked fiber laser at the central wavelength of 1547 nm [45]. Different from previous work that used high-quality nanosheet-based TIs as mode-lockers, they used bulk-structured $Bi_2Te_3$ fabricated by ME and finally obtained 600-fs pulses with an average output power of 0.8 mW. The results illustrated that the bulk-structured TI could also be an efficient mode-locker with the advantages of low cost and easy fabrication. After that, Liu et al. used a $Bi_2Se_3$-PVA composite as SA in an anomalous dispersion fiber ring laser and achieved femtosecond mode-locked pulses of ~660 fs with an SNR more than 55 dB, indicating its high stability [46].

Sotor et al. reported on the first stretched-pulse mode-locked laser based on TIs. In this work, they deposited bulk $Sb_2Te_3$ on the side-polished fiber and spliced it to a dispersion-managed laser resonator, which generated 128-fs pulses with an average output power of 1 mW [47]. In 2015, Yan et al. proposed a passive harmonic mode-locked fiber laser operating at 1562.4 nm enabled by a $Bi_2Te_3$ film SA, where the microfiber-based TI SA was fabricated by the PLD method for the first time [48]. As a result, stable fundamental mode-locking was demonstrated with a pulse width of 320 fs and an output power of 45.3 mW at the repetition rate of 2.95 GHz.

In 2015, the dissipative solitons operation of a fiber laser based on $Sb_2Te_3$ was proposed by Boguslawski et al. for the first time, which possessed a central wavelength of 1558 nm with a pulse duration of 167 fs and pulse energy of 0.21 nJ [49]. In 2019, Wei et al. reported a passively mode-locked all-fiber EDFL based on CVD-grown $Bi_2Te_3$ film with the maximum output power, as well as pulse energy of 40.37 mW and 23.9 nJ [50]. Later, Guo et al. employed CVD-grown $Bi_2Se_3$ as SA in a bidirectional pumped laser cavity, raising the parameters to 82.6 mW and 48.3 nJ [51] and 185.3 mW and 171.3 nJ [52], successively. The improvement of the parameters validated that CVD-grown $Bi_2Se_3$ exhibits a remarkable capability in high power mode-locked lasers.

In 2013, Luo et al. proposed the first passively Q-switched YDFL based on $Bi_2Se_3$ at 1067 nm, indicating that TIs SAs had come on the stage in ultrafast lasers at 1 μm [53]. In 2014, Li et al. achieved both Q-switched and Q-switched mode-locked operation in a solid-state laser in 1-μm band by using a $Bi_2Te_3$ SA mirror, obtaining the maximum output power of 183 and 247 mW, respectively [54]. Shortly afterward, Chi et al. reported on the generation of all-normal-dispersion dissipative-soliton pulses with a bulk $Bi_2Te_3$ at 1.06 μm [55]. At a repetition rate of 1.44 MHz, stable mode-locked pulses had a pulse duration of 230 ps. Equally important is that Dou et al. also exploited $Bi_2Se_3$ as SA in an all-normal-dispersion YDFL, which possessed a pulse width of 46 ps and maximum average output power of 33.7 mW at 44.6 MHz [56].

In 2015, Xu et al. achieved Q-switched operation at 1313 nm by using LPE-prepared $Bi_2Se_3$ nanosheets as SA and Nd:$LiYF_4$ (YLF) crystals as the gain medium, obtaining pulse energy up to 1.23 μJ at a repetition rate of 161.3 kHz [57]. Later, Xu et al. proposed passively Q-switched mode-locked Nd:yttrium vanadate lasers enabled by large-size $Bi_2Te_3$ sheets at 1064 and 1342 nm separately both with a short pulse duration of a nanosecond, revealing the promising application of large-size $Bi_2Te_3$ in high-energy short pulse generation [58].

In 2018, Wang et al. demonstrated an all-solid-state mode-locked laser based on a large-area $Bi_2Te_3$ SA mirror prepared by the spinning coating-co-reduction approach (SCCA), which had a repetition rate up to 1 GHz, output power up to 180 mW, and SNR of 61 dB [59]. These results indicates that TIs could be potential SAs in solid-state lasers for the generation of highly stable ultrafast pulses.

In 2014, Luo et al. employed TIs as SA in a Q-switched TDFL at 1.98 μm for the first time, where TI-$Bi_2Se_3$ nanosheets were prepared by the LPE method [60]. Later, the first mode-locked fiber laser based on $Bi_2Te_3$ in the 2-μm region was obtained by Jung et al. [61]. They utilized the bulk-structured $Bi_2Te_3$ prepared by ME and achieved 795-fs pulses at a repetition rate of 27.9 MHz. In 2015, Yin et al. demonstrated the generation of stable bunched solitons and harmonically mode-locked solitons in a $Bi_2Te_3$-based mode-locked THDFL, obtaining a pulse duration of 1.26 ps at a repetition rate of 21.5 MHz [62].

Compared with $Bi_2Te_3$, the other commonly used TI ($Bi_2Se_3$) was applied to mode-locked fiber lasers in 2 μm very late until 2018, when Lee et al. proposed a mode-locked THDFL enabled by a bulk-structured $Bi_2Se_3$ with a pulse duration of ~853 fs [63]. In the same year, Loiko et al. demonstrated a Q-switched thulium-doped gadolinium vanadate laser based on a $Sb_2Te_3$ film that was fabricated by the MSD method, obtaining a maximum average output power of 0.70 W at the repetition rate of ~200 kHz [64].

In 2015, Yin et al. reported on the first mid-IR fiber laser mode-locked by $Bi_2Te_3$ SA mirror at 2830 nm with a pulse duration of ~6 ps and maximum pulse energy up to 8.6 nJ [65]. Li et al. achieved passively Q-switched operation in a Ho-doped $ZrF_4$-$BaF_2$-$LaF_3$-$AlF_3$-NaF (ZBLAN) fiber laser induced by $Bi_2Te_3$ SA, which produced high-energy pulses with a maximum output power of 327.4 mW and pulse energy of 3.99 μJ [66]. This work indicated that TIs could be reliable SAs for mid-IR pulse generation.

In 2016, Tang et al. demonstrated a Q-switched Er-doped ZBLAN fiber laser by utilizing $Bi_2Te_3$ as SA, which possessed an average power up to 856 mW at the repetition rate of 92 kHz [67]. In 2018, Li et al. reported on a miniaturized all-fiber Ho-doped fiber laser (HDFL) Q-switched by $Bi_2Se_3$ nanosheets, in which the shortest pulse duration was 1.54 μs at the maximum output power of 315 μW [68].

As another 2D material widely applied in ultrafast photonics right after graphene, TIs enjoy various merits, including broadband saturable absorption properties, a large nonlinear refractive index, and an innate giant modulation depth (up to 95%) [40][69][70]. Therefore, TIs have been considered as remarkable SAs for the generation of ultrashort, high energy, and high repetition rate pulses within a wide wavelength ranging from visible to mid-IR regions [50][71][72][73]. However, the relatively slow relaxation time, complicated fabrication process, and relatively low mode-locking stability limit the applications of TIs in ultrafast photonics [74][37][75].

In addition, although $Sb_2Te_3$ SA demonstrated reliable performance in ultrashort and high power pulses generation [76][77], the majority of applications focus on the telecommunication band. Hence, it is worthwhile to explore more operating wavelengths of $Sb_2Te_3$ SA. Apart from that, more fabrication methods for TIs with lower cost and easier manipulation, as well as applications in a higher wavelength band of mid-IR region also need to be further studied.

## 3. Transition Metal Dichalcogenides

Since Wang et al. investigated the excellent saturable absorption properties of $MoS_2$ at 800 nm [78], TMDs, such as $MoS_2$, $MoSe_2$, $WS_2$, and $WSe_2$, have come to the stage of ultrafast photonics applications. In 2014, Zhang et al. first reported on a mode-locked fiber laser at 1054.3 nm with a pulse width of 800 ps, in which a few-layer $MoS_2$ film was fabricated through the hydrothermal exfoliation method [79]. Later, the first Q-switched fiber laser based on a $MoS_2$-polymer composite SA was demonstrated by Woodward et al. obtaining a typical Q-switched pulse operated at 1068.2 nm with a pulse width of 2.7 μs [80]. Xu et al. realized a Q-switched solid-state laser by employing LPE-prepared $MoS_2$ nanosheets in an Nd:yttrium aluminum perovskite (Nd:YAP) laser cavity, where high energy pulses with a peak power of 4.92 W were generated, revealing the promising potential of $MoS_2$ SA for ultrafast solid-state lasers [81].

In 2015, Zhao et al. proposed a simple chemical weathering-assisted exfoliation method to fabricate $MoS_2$ and $WS_2$ monolayers, which exhibited extraordinary performance in Q-switched and mode-locked all-solid-state lasers [82]. Based on this fabrication method, Hou et al. further disposed $WS_2$ through ultrasonic treatment and used it as SA to obtain a mode-locked Yb:YAG laser with a pulse duration of 736 fs at a repetition rate of 86.7 MHz, further proving that $WS_2$ could be an excellent SA for ultrafast solid-state lasers [83]. In the same year, Lin et al. demonstrated the first tunable Q-switched YDFL based on $WS_2$ that prepared by the intercalation method, and the SEM image is shown in **Figure 3**a [84]. As shown in **Figure 3**b–d, the typical Q-switched pulses operated at 1048.1 nm with a pulse duration of 1.65 μs and an SNR of ~50 dB at the repetition rate of 81.5 kHz.

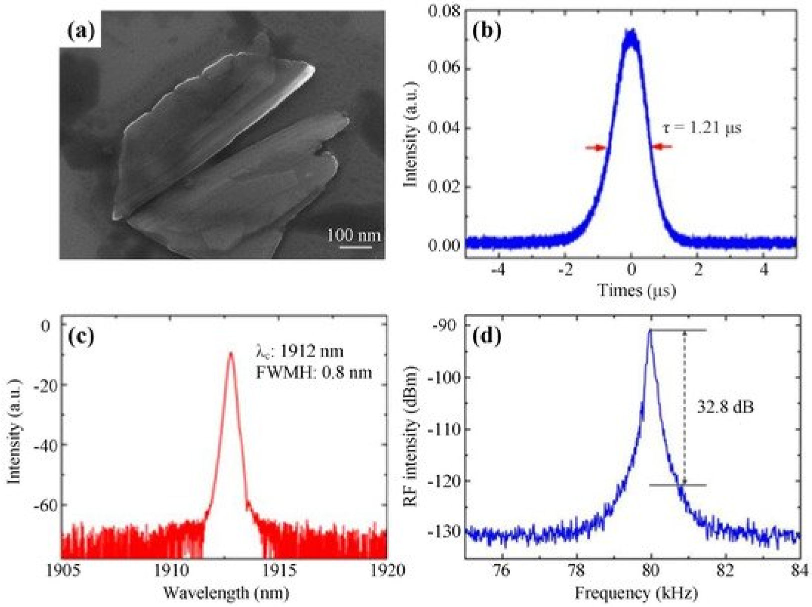


**Figure 3.** The experimental results of Q-switched YDFL enabled by $WS_2$ SA. (**a**) SEM image of $WS_2$ nanoplates. (**b**) Output spectrum, (**c**) single pulse profile, and (**d**) radio frequency (RF) spectrum at the repetition rate of 81.5 kHz. (**a**–**d**) adapted from [84].

In 2016, Cheng et al. reported on waveguide Nd:YAG lasers passively Q-switched by CVD-grown $MoSe_2$ and $WSe_2$ respectively, both achieving nanosecond pulse durations [85]. Adopting almost the same scheme, Wang et al. realized Q-switched Nd:YAG lasers based on $WS_2$ solution of different concentrations [86]. By changing the concentrations of the $WS_2$ solutions, they uncovered that the pulse width decreased and the repetition rate rose along with the increase of concentration.

In 2014, Liu et al. demonstrated a femtosecond mode-locked fiber laser at 1569.5 nm with a pulse duration of 710 fs, and a repetition rate of 12.09 MHz by exploiting a firmly $MoS_2$-PVA composite as SA, which was the first application of $MoS_2$ SA in a telecommunication band [87]. Following this work, Liu et al. realized a high-order passively harmonic EDFL mode-locked by microfiber-based $MoS_2$ SA [88]. According to the results, the laser achieved highest harmonic order of 369th at the repetition rate of 2.5 GHz. Soon after that, stable Q-switched operation based on $MoS_2$ with a widely tunable waveband from 1519.6 to 1567.7 nm was achieved by Huang et al. which possessed a maximum pulse energy of 160 nJ and an SNR of 50 dB [89].

Considering the defect of the polymer binder for decreasing the damage threshold, Khazaeizhad et al. coated the $MoS_2$ film on a side-polished fiber to fabricate a polymer-free $MoS_2$ SA. They used it to obtain not only dissipative soliton pulse trains with a bandwidth of 23.2 nm in the normal dispersion regime but also soliton-like pulses of 637 fs in the anomalous dispersion regime [90]. In addition to $MoS_2$, $WS_2$ is also used as a SA for generating ultrashort pulses. In 2015, Mao et al. uncovered the ultrafast saturable absorption property of $WS_2$ nanosheets with the merit of a high damage threshold and used it as SA to achieve stable soliton mode-locking [91]. In pace with this work, stable Q-switched and femtosecond mode-locked operation in the EDFL based on LPE-grown $WS_2$ were also reported by Kassani et al. and Khazaeinezhad et al. separately [92][93].

Yan et al. realized a harmonic mode-locked EDFL by inserting $WS_2$ film-SA synthesized through the PLD method, where the 53rd harmonic with a pulse width of 452 fs and an SNR of 65 dB was obtained at the repetition rate of 1.04 GHz [94]. This work revealed that $WS_2$ could be an outstanding mode-locker and Q-switcher in ultrafast photonics. In the same year, $MoSe_2$ was first exploited as SA in 1.5 μm by Luo et al. who embedded few-layer $MoSe_2$ in a polymer composite and achieved mode-locked soliton pulses with a pulse duration of 1.45 ps [95]. In 2016, Koo et al. utilized a $MoSe_2$-PVA composite to demonstrate a femtosecond harmonic mode-locked fiber laser with a maximum harmonic order of 212th at the repetition rate of 3.27 GHz, which is the largest repetition rate achieved by 2D material-based lasers to date [96].

In 2017, Liu et al. transferred PLD-prepared $WS_2$ on a small waist diameter tapered fiber along with a long fused zone covered by a gold film to obtain a SA that had a large modulation depth [97]. Thus, highly stable pulses with an SNR up to 93 dB and a pulse duration of 67 fs were obtained, which was the shortest pulse duration achieved in mode-locked fiber lasers based on TMDs, confirming the promising future of $WS_2$ in ultrashort pulse generation. In 2018, a Q-switched EDFL based on CVD-grown $MoSe_2$ was reported by Liu et al. which emitted 207-fs pulses with an SNR of 85 dB, further indicating that the combination of the CVD method and the tapered fiber structure is conducive to fabricate high performance SAs for the generation of stable ultrashort pulses [98].

In 2014, by introducing suitable defects in the process, Wang et al. fabricated a type of few-layered $MoS_2$ with large broadband saturable absorption extending to 2.4 μm [99]. The $MoS_2$ was applied to demonstrate Q-switching in solid-state lasers at 1.06, 1.42, and 2.1 μm separately. Later, Luo et al. reported on broadband Q-switched fiber lasers by using a few-layer $MoS_2$-PVA composite SA at different wavelengths, where the span of the wavelengths covered from 1 to 2 μm [100]. Their work indicated unambiguously that few-layer $MoS_2$ was a promising broadband SA. In 2015, Kong et al. realized both Q-switching and Q-switched mode-locking in a Tm:CLNGG laser induced by $MoS_2$ golden mirror SA [101].

Subsequently, the first mode-locked operation based on $MoS_2$ in 2 μm was achieved by Tian et al., who obtained a pulse energy of 15.5 nJ and a repetition rate of 9.67 MHz [102]. In the same year, Jung et al. proposed the first application of $WS_2$ in an ultrafast mode-locked fiber laser at 1941 nm with an SNR up to 72 dB [103]. In 2017, Lee et al. achieved a femtosecond mode-locked fiber laser at 1912 nm based on $MoSe_2$-PVA composite SA with a pulse duration of ~920 fs and a repetition rate of 18.21 MHz [104]. Another relatively typical TMD, $WSe_2$, was not used as a SA in the 2-μm region until 2018 by Wang et al., who demonstrated mode-locked soliton pulses had a pulse duration of 1.16 ps and an average output power of 32.5 mW at a repetition rate of 11.36 MHz [105].

In 2016, TMD SA started to be applied in the 3-μm region. Fan et al. reported on a Q-switched Er:lutetium oxide ($Er:Lu_2O_3$) laser at the central wavelength of 2.84 μm induced by a few-layer $MoS_2$-based SA, which possessed a repetition rate of 121 kHz and pulse energy of 8.5 μJ, corresponding to a Watt-level average output power of 1.03 W [106]. Subsequently, Wei et al. achieved Q-switched operation in a fiber laser based on $WS_2$ at 2865.7 nm [107]. The above are the early demonstrations of TMD SA for Q-switching in 3 μm, which indicated the potential of TMD SA applied in the mid-IR region.

In the next two years, Q-switched solid-state lasers in 3 μm based on $MoS_2$ and $WSe_2$ were demonstrated by Zhang and Liu et al. successively [108][109]. In 2020, Guo et al. achieved mode-locked operation based on CVD-grown $WSe_2$ SA mirror at 2789.6 nm with a maximum average output power of 360 mW and a repetition rate of 42.43 MHz, which is the first time TMD severed as mode-locker in the 3-μm region [110].

Many merits of TMDs, such as layer-dependent bandgap and broadband operation, enable them as outstanding SAs from the visible to mid-IR regions [94][99], especially in the Q-switched operation [37][111]. However, the relatively large direct bandgap and low optical damage threshold limit the applications in long operating wavelength as well as in high power lasers [112]. Additionally, the commonly used methods for integrating TMD SAs thus far are either complex and difficult, or induce additional insertion loss to the cavity, which is worthy of optimization to achieve more fruitful results in the mid-IR region.

For example, Liu et al. prepared a $WS_2/SiO_2$ SA by the sol-gel method to overcome the shortcomings of scattering loss and a low optical damage threshold, as well as to achieve long-term stable mode-locked pulses under high power operation [113]. Furthermore, although $MoS_2$, $MoSe_2$, $WS_2$, and $WSe_2$ have been widely studied and applied, other TMDs, such as $SnS_2$, $SnSe_2$, and platinum diselenide, which show exceptional excellent properties, also deserve more investigation regarding ultrafast photonics [114][115][116][117][118].

## 4. Black Phosphorus

After the broadband nonlinear optical response of BP was reported in 2015 [36], Chen et al. utilized BP as SA to realize not only mode-locking at 1571.45 nm with a pulse duration down to 946 fs but also Q-switching at 1562.87 nm with a maximum pulse energy of 94.3 nJ [74]. Later, Li et al. achieved mode-locked operation based on BP with a pulse duration of 786 fs and Q-switched operation with a maximum pulse energy of 18 nJ in the telecommunication band [119]. They also studied the linear and nonlinear absorption properties of BP and found that it was polarization and thickness dependent.

In 2016, Chen et al. demonstrated the generation of stable mode-locked soliton pulses with a tunable wavelength extending from 1549 to 1575 nm by incorporating LPE-prepared BP into an all anomalous dispersion Er-doped cavity [120]. In the same year, Song et al. achieved a vector soliton fiber laser mode-locked by BP for the first time, where the LPE-prepared BP nanoflakes were transferred onto the end facet of a fiber [121]. According to the results, stable 670-fs soliton pulses centered at ~1550 nm were obtained with a fundamental repetition rate of 8.77 MHz and an SNR of ~60 dB.

In 2017, a dual-wavelength mode-locked vector soliton fiber laser based on few-layer BP centered at 1533 and 1558 nm with a pulse duration of ~700 fs was proposed by Yun et al. which validated the potential of BP SA for ultrafast vector soliton generation [122]. In 2018, Jin et al. obtained stable stretched pulses in a mode-locked EDFL based on inkjet-printed BP with a shorter pulse duration of 102 fs and a wider bandwidth of 40 nm compared with previous reports. According to the results, the SNR was up to 60 dB, and the stable mode-locked operation could be maintained for a long time (>10 days), which indicated that the laser experiences long-term stability [123].

In 2015, Zhang et al. reported on a mode-locked solid-state laser based on BP SA mirror at 1064.1 nm with a pulse width of 6.1 ps and average output power of 460 mW [124]. In the same year, Ma et al. realized the first Q-switched solid-state laser enabled by BP at the central wavelength of 1046 nm where passively Q-switched pulses had an average output power of 37 mW at the maximum repetition rate of 113.6 kHz, corresponding to a pulse energy of ~325.7 nJ [125]. Their works opened the way for BP SA in applications of ultrafast lasers in 1 μm.

In 2016, Al-Masoodi et al. demonstrated Q-switched operation in a BP-based YDFL, achieving a pulse energy of 328 nJ at the repetition rate of 32.9 kHz [126]. Then, Su et al. obtained femtosecond pulses of 272 fs in a solid-state laser mode-locked by BP for the first time with the maximum average output power as high as 0.82 W [127]. Rashidet et al. proposed a dual-wavelength Q-switched laser with a BP thin film operated at 1038.68 and 1042.05 nm [128]. In addition, Ahmad et al. proposed a wavelength-tunable BP-based Q-switched fiber laser at an operational wavelength ranging from 1056.6 to 1083.3 nm [129].

In 2017, Huang et al. achieved a Q-switched laser at 1064 nm where microfibers were sandwiched by BP flakes to integrate SA, providing an effective way to prolong the life of BP flakes by isolating them from the air [130]. In 2019, Wang et al. demonstrated both Q-switched and mode-locked lasers based on BP by inserting polarization-maintaining fiber Bragg gratings [131]. The operating wavelength could be turned to 1063.8 and 1064.1 nm, respectively, as well as concurrently.

Following the initial applications in 1 μm, BP began to be used in the eye-safe region of 2 μm. In 2015, Sotor et al. first reported on a mode-locked fiber laser enabled by mechanically exfoliated BP films at 1910 nm with a pulse duration of 739 ps and an average output power of 1.5 mW at a repetition rate of 36.8 MHz [132]. In 2016, Yu et al. achieved the first

Q-switched operation in 2 μm based on BP with the shortest pulse width of 731 ns. **Figure 4**a shows the SEM image of the LPE-prepared BP. As shown in **Figure 4**b–d, the laser produced 1.21-μs pulses with the central wavelength of 1912 nm and an SNR of 32.8 dB at the repetition rate of 79.8 kHz [133].

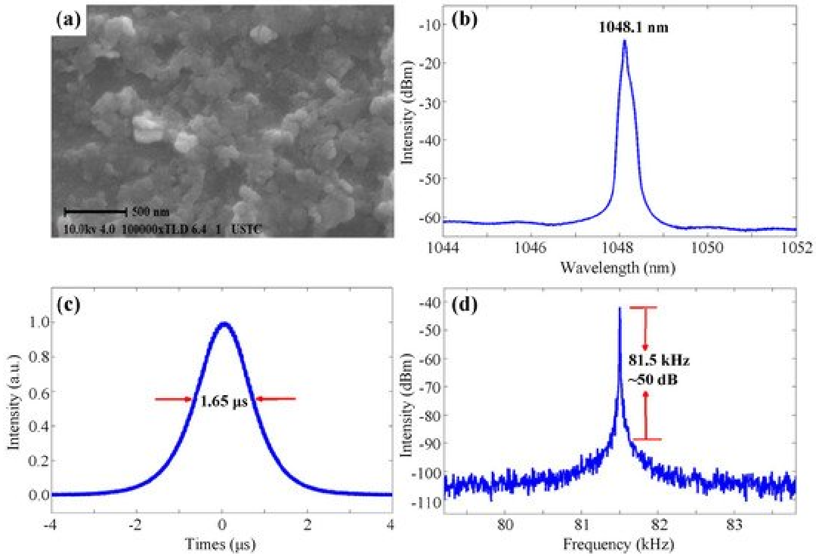


**Figure 4.** The experimental results of Q-switched THDFL enabled by BP SA. (**a**) SEM image of LPE-grown BP nanoplatelets. (**b**) Single pulse profile, (**c**) output spectrum, and (**d**) RF spectrum at a repetition rate of 113.3 kHz. (**a**–**d**) adapted from [133].

Later, the earliest solid-state laser Q-switched by BP in 2 μm was demonstrated by Chu et al., who achieved the shortest pulse duration of 1.78 μs at the repetition rate of 19.25 kHz, corresponding to a pulse energy of 7.84 μJ [134]. Then, Zhang et al. reported on a dual-wavelength Q-switched Tm:YAP bulk laser operating at 1969 and 1979 nm, which further proved the capability of BP for Q-switched operation in 2 μm [135]. When it came to 2017, Pawliszewska et al. proposed the first use of BP SA as a mode-locker in HDFL, where harmonic operation up to 10th order was demonstrated with a pulse duration of 1.3 ps at the repetition rate of 290 MHz [136].

In 2015, Qin et al. demonstrated Q-switched operation at 2.8 μm based on a BP SA mirror for the first time obtaining a maximum average output power of 485 mW and pulse energy of 7.7 μJ [137]. Without stopping, in the next year, they adopted the same method to fabricate BP SA and obtained a mode-locked Er-doped ZBLAN fiber laser with a pulse duration of 42 ps and a repetition rate of 24 MHz, which promoted the applications of BP as SA for ultrafast lasers in the mid-IR region [138]. In 2016, Kong et al. reported on a BP-based Q-switched Er:$Y_2O_3$ ceramic laser at 2.72 μm with a pulse energy of 0.48 μJ at 12.6 kHz [139].

Soon after that, Li et al. inserted LPE-prepared BP into rare earth ion doped fluoride fiber lasers to realize mode-locked and Q-switched operation, respectively, thus, further enhancing the working wavelength of BP-based fiber lasers [140]. In the same year, a dual-wavelength Q-switched solid-state laser at 2.79 μm was demonstrated by Liu et al. [141]. They adopted BP nanoflakes as SA in an Er:strontium fluoride (Er:$SrF_2$) bulk laser that generated 702-ns pulses at a repetition rate of 77.03 kHz.

In 2018, Qin et al. demonstrated both mode-locked and Q-switched lasers in 3.5 μm enabled by BP SA, which was the first time mode-locking and Q-switching are operated in such a high spectral region, validating the superb potential of BP as SA in the mid-IR region. In 2019, Woodward et al. reported on a dysprosium-doped fiber laser Q-switched by BP SA with a tunable wavelength from 2.97 to 3.32 μm by using an acousto-optic tunable filter [142].

Benefiting from the layer-dependent direct bandgap that can be broadly turned from ~0.3 (bulk) to ~2 eV (monolayer), BP stands out as an excellent filler between zero-bandgap graphene and wide-bandgap TMDs [143][144][145]. Although BP can be fabricated conveniently with low cost [137], its instability in air and water molecules requires relatively strict conditions for its preparation and operation, which restricts the application especially in high power regimes [146][147][148]. For now, there is a need for more research on not only economic fabrication methods for stable BP SA but also its application in certain types of ultrafast lasers; for example, harmonic mode-locked lasers with high repetition rate pulses, which possess critical applications in optical communication [149], spectroscopy [150], and frequency bombing [151].

## References


1. Hasan, T.; Sun, Z.; Wang, F.; Bonaccorso, F.; Tan, P.H.; Rozhin, A.G.; Ferrari, A.C. Nanotube polymer composites for ul trafast photonics. Adv. Mater. 2009, 21, 3874–3899.
2. Bao, Q.; Zhang, H.; Wang, Y.; Ni, Z.; Yan, Y.; Shen, Z.X.; Loh, K.P.; Tang, D.Y. Atomic-layer graphene as a saturable ab sorber for ultrafast pulsed lasers. Adv. Funct. Mater. 2009, 19, 3077–3083.
3. Zhang, H.; Bao, Q.; Tang, D.; Zhao, L.; Loh, K. Large energy soliton erbium-doped fiber laser with a graphene-polymer composite mode locker. Appl. Phys. Lett. 2009, 95, 141103.
4. Wang, C.; Liu, J.; Zhang, H. Ultrafast pulse lasers based on two-dimensinal nanomaterials. Acta Phys. Sin. 2019, 68, 1 88101.
5. Sun, Z.; Popa, D.; Hasan, T.; Torrisi, F.; Wang, F.; Kelleher, E.J.R.; Travers, J.C.; Nicolosi, V.; Ferrari, A.C. A stable, wid eband tunable, near transform-limited, graphene-mode-locked, ultrafast laser. Nano Res. 2010, 3, 653–660.
6. Shang, C.; Zhang, Y.; Qin, H.; He, B.; Zhang, C.; Sun, J.; Li, J.; Ma, J.; Ji, X.; Xu, L.; et al. Review on wavelength-tunab le pulsed fiber lasers based on 2D materials. Opt. Laser Technol. 2020, 131, 106375.
7. Guo, B.; Xiao, Q.L.; Wang, S.H.; Zhang, H. 2D layered materials: Synthesis, nonlinear optical properties, and device ap plications. Laser Photonics Rev. 2019, 13, 1800327.
8. Luo, Z.; Zhou, M.; Weng, J.; Huang, G.; Xu, H.; Ye, C.; Cai, Z. Graphene-based passively Q-switched dual-wavelength erbium-doped fiber laser. Opt. Lett. 2010, 35, 3709–3711.
9. Popa, D.; Sun, Z.; Hasan, T.; Torrisi, F.; Wang, F.; Ferrari, A.C. Graphene Q-switched, tunable fiber laser. Appl. Phys. L ett. 2011, 98, 073106.
10. Duarte, F.J. Tunable Laser Applications; CRC Press: Boca Raton, FL, USA, 2008; Volume 150.
11. Olesberg, J.T.; Arnold, M.A.; Mermelstein, C.; Schmitz, J.; Wagner, J. Tunable laser diode system for noninvasive blood glucose measurements. Appl. Spectrosc. 2005, 59, 1480–1484.
12. Besson, J.P.; Schilt, S.; Thévenaz, L. Multi-gas sensing based on photoacoustic spectroscopy using tunable laser diod es. Spectrochim. Acta Part A 2004, 60, 3449–3456.
13. Gao, C.; Wang, R.; Zhu, L.; Gao, M.; Wang, Q.; Zhang, Z.; Wei, Z.; Lin, J.; Guo, L. Resonantly pumped 1.645 μm high r epetition rate Er:YAG laser Q-switched by a graphene as a saturable absorber. Opt. Lett. 2012, 37, 632–634.
14. Sobon, G.; Sotor, J.; Abramski, K.M. Passive harmonic mode-locking in Er-doped fiber laser based on graphene satura ble absorber with repetition rates scalable to 2.22 GHz. Appl. Phys. Lett. 2012, 100, 161109.
15. Fu, B.; Gui, L.; Zhang, W.; Xiao, X.; Zhu, H.; Yang, C. Passive harmonic mode locking in erbium-doped fiber laser with graphene saturable absorber. Opt. Commun. 2013, 286, 304–308.
16. Di Dio Cafiso, D.S.; Ugolotti, E.; Schmidt, A.; Petrov, V.; Griebner, U.; Agnesi, A.; Cho, W.B.; Jung, B.H.; Rotermund, F.; Bae, S.; et al. Sub-100-fs Cr:YAG laser mode-locked by monolayer graphene saturable absorber. Opt. Lett. 2013, 38, 1 745–1747.
17. Sotor, J.; Pasternak, I.; Krajewska, A.; Strupinski, W.; Sobon, G. Sub-90 fs a stretched-pulse mode-locked fiber laser ba sed on a graphene saturable absorber. Opt. Express 2015, 23, 27503–27508.
18. Fu, B.; Li, J.; Cao, Z.; Popa, D. Bound states of solitons in a harmonic graphene-mode-locked fiber laser. Photon. Res. 2019, 7, 116–120.
19. Yu, H.; Chen, X.; Zhang, H.; Xu, X.; Hu, X.; Wang, Z.; Wang, J.; Zhuang, S.; Jiang, M. Large energy pulse generation modulated by graphene epitaxially grown on silicon carbide. ACS Nano 2010, 4, 7582–7586.
20. Zhao, L.M.; Tang, D.Y.; Zhang, H.; Wu, X.; Bao, Q.; Loh, K.P. Dissipative soliton operation of an ytterbium-doped fiber l aser mode locked with atomic multilayer graphene. Opt. Lett. 2010, 35, 3622–3624.
21. Liu, J.; Wu, S.; Yang, Q.H.; Wang, P. Stable nanosecond pulse generation from a graphene-based passively Q-switche d Yb-doped fiber laser. Opt. Lett. 2011, 36, 4008–4010.
22. Cho, W.B.; Kim, J.W.; Lee, H.W.; Bae, S.; Hong, B.H.; Choi, S.Y.; Baek, I.H.; Kim, K.; Yeom, D.I.; Rotermund, F. High-q uality, large-area monolayer graphene for efficient bulk laser mode-locking near 1.25 μm. Opt. Lett. 2011, 36, 4089–40 91.
23. Zhao, N.; Liu, M.; Liu, H.; Zheng, X.W.; Ning, Q.Y.; Luo, A.P.; Luo, Z.C.; Xu, W.C. Dual-wavelength rectangular pulse Yb -doped fiber laser using a microfiber-based graphene saturable absorber. Opt. Express 2014, 22, 10906–10913.
24. Wang, Q.; Teng, H.; Zou, Y.; Zhang, Z.; Li, D.; Wang, R.; Gao, C.; Lin, J.; Guo, L.; Wei, Z. Graphene on SiC as a Q-swit cher for a 2 μm laser. Opt. Lett. 2012, 37, 395–397.

25. Ma, J.; Xie, G.Q.; Lv, P.; Gao, W.L.; Yuan, P.; Qian, L.J.; Yu, H.H.; Zhang, H.J.; Wang, J.Y.; Tang, D.Y. Graphene mode-locked femtosecond laser at 2 µm wavelength. Opt. Lett. 2012, 37, 2085–2087.

26. Zhang, M.; Kelleher, E.; Torrisi, F.; Sun, Z.; Hasan, T.; Popa, D.; Wang, F.; Ferrari, A.; Popov, S.; Taylor, J. Tm-doped fiber laser mode-locked by graphene-polymer composite. Opt. Express 2012, 20, 25077–25084.

27. Liu, J.; Xu, J.; Wang, P. Graphene-based passively Q-switched 2µm thulium-doped fiber laser. Opt. Commun. 2012, 285, 5319–5322.

28. Fu, B.; Gui, L.; Li, X.; Xiao, X.; Zhu, H.; Yang, C. Generation of 35-nJ nanosecond pulse from a passively mode-locked Tm, Ho-codoped fiber laser With graphene saturable absorber. IEEE Photonics Technol. Lett. 2013, 25, 1447–1449.

29. Jiang, M.; Ma, H.F.; Ren, Z.Y.; Chen, X.M.; Long, J.Y.; Qi, M.; Shen, D.Y.; Wang, Y.S.; Bai, J.T. A graphene Q-switched nanosecond Tm-doped fiber laser at 2 µm. Laser Phys. Lett. 2013, 10, 79–83.

30. Zhao, T.; Wang, Y.; Chen, H.; Shen, D. Graphene passively Q-switched Ho:YAG ceramic laser. Appl. Phys. B 2014, 116, 947–950.

31. Fu, B.; Hua, Y.; Xiao, X.; Zhu, H.; Sun, Z.; Yang, C. Broadband graphene saturable absorber for pulsed fiber lasers at 1, 1.5, and 2 µm. IEEE J. Sel. Top. Quantum Electron. 2014, 20, 411–415.

32. Cizmeciyan, M.N.; Kim, J.W.; Bae, S.; Hong, B.H.; Rotermund, F.; Sennaroglu, A. Graphene mode-locked femtosecond Cr:ZnSe laser at 2500 nm. Opt. Lett. 2013, 38, 341–343.

33. Tokita, S.; Murakami, M.; Shimizu, S.; Hashida, M.; Sakabe, S. Graphene Q-switching of a 3 µm Er:ZBLAN fiber laser. In Proceedings of the Advanced Solid State Lasers, Optical Society of America, Paris, France, 27 October–1 November 2013; p. AF2A.9.

34. Zhu, G.; Zhu, X.; Wang, F.; Xu, S.; Li, Y.; Guo, X.; Balakrishnan, K.; Norwood, R.A.; Peyghambarian, N. Graphene mode-locked fiber laser at 2.8 µm. IEEE Photonics Technol. Lett. 2016, 28, 7–10.

35. Pushkin, A.V.; Migal, E.A.; Tokita, S.; Korostelin, Y.V.; Potemkin, F.V. Femtosecond graphene mode-locked Fe:ZnSe laser at 4.4 microm. Opt. Lett. 2020, 45, 738–741.

36. Lu, S.B.; Miao, L.L.; Guo, Z.N.; Qi, X.; Zhao, C.J.; Zhang, H.; Wen, S.C.; Tang, D.Y.; Fan, D.Y. Broadband nonlinear optical response in multi-layer black phosphorus: An emerging infrared and mid-infrared optical material. Opt. Express 2015, 23, 11183–11194.

37. Fu, B.; Sun, J.; Wang, G.; Shang, C.; Ma, Y.; Ma, J.; Xu, L.; Scardaci, V. Solution-processed two-dimensional materials for ultrafast fiber lasers (invited). Nanophotonics 2020, 9, 2169–2189.

38. Xu, J.; Liu, J.; Wu, S.; Yang, Q.H.; Wang, P. Graphene oxide mode-locked femtosecond erbium-doped fiber lasers. Opt. Express 2012, 20, 15474–15480.

39. Zhao, C.; Zou, Y.; Chen, Y.; Wang, Z.; Lu, S.; Zhang, H.; Wen, S.; Tang, D. Wavelength-tunable picosecond soliton fiber laser with Topological Insulator: Bi2Se3 as a mode locker. Opt. Express 2012, 20, 27888–27895.

40. Zhao, C.; Zhang, H.; Qi, X.; Chen, Y.; Wang, Z.; Wen, S.; Tang, D. Ultra-short pulse generation by a topological insulator based saturable absorber. Appl. Phys. Lett. 2012, 101, 211106.

41. Zhang, H.; Liu, C.X.; Qi, X.L.; Dai, X.; Fang, Z.; Zhang, S.C. Topological insulators in Bi2Se3, Bi2Te3 and Sb2Te3 with a single Dirac cone on the surface. Nat. Phys. 2009, 5, 438–442.

42. Bernard, F.; Zhang, H.; Gorza, S.P.; Emplit, P. Towards mode-locked fiber laser using topological insulators. In Proceedings of the Advanced Photonics Congress, Optical Society of America, Colorado Springs, CO, USA, 17–21 June 2012; OSA Technical Digest (online). p. NTh1A.5.

43. Pinghua, T.; Xiaoqi, Z.; Chujun, Z.; Yong, W.; Han, Z.; Deyuan, S.; Shuangchun, W.; Dingyuan, T.; Dianyuan, F. Topological insulator: Bi2Te3 saturable absorber for the passive Q-switching operation of an in-band pumped 1645-nm Er:YAG ceramic laser. IEEE Photonics J. 2013, 5, 1500707.

44. Chen, Y.; Zhao, C.; Huang, H.; Chen, S.; Tang, P.; Wang, Z.; Lu, S.; Zhang, H.; Wen, S.; Tang, D. Self-assembled topological insulator: Bi2Se3 membrane as a passive Q-switcher in an erbium-doped fiber laser. J. Light. Technol. 2013, 31, 2857–2863.

45. Lee, J.; Koo, J.; Jhon, Y.M.; Lee, J.H. A femtosecond pulse erbium fiber laser incorporating a saturable absorber based on bulk-structured Bi2Te3 topological insulator. Opt. Express 2014, 22, 6165–6173.

46. Liu, H.; Zheng, X.W.; Liu, M.; Zhao, N.; Luo, A.P.; Luo, Z.C.; Xu, W.C.; Zhang, H.; Zhao, C.J.; Wen, S.C. Femtosecond pulse generation from a topological insulator mode-locked fiber laser. Opt. Express 2014, 22, 6868–6873.

47. Sotor, J.; Sobon, G.; Abramski, K.M. Sub-130 fs mode-locked Er-doped fiber laser based on topological insulator. Opt. Express 2014, 22, 13244–13249.

48. Yan, P.; Lin, R.; Ruan, S.; Liu, A.; Chen, H. A 2.95 GHz, femtosecond passive harmonic mode-locked fiber laser based on evanescent field interaction with topological insulator film. Opt. Express 2015, 23, 154–164.

49. Boguslawski, J.; Sobon, G.; Zybala, R.; Sotor, J. Dissipative soliton generation in Er-doped fiber laser mode-locked by Sb2Te3 topological insulator. Opt. Lett. 2015, 40, 2786–2789.

50. Wei, Q.; Niu, K.; Han, X.; Zhang, H.; Zhang, C.; Yang, C.; Man, B. Large energy pulses generation in a mode-locked Er-doped fiber laser based on CVD-grown Bi2Te3 saturable absorber. Opt. Mater. Express 2019, 9, 3535–3545.

51. Guo, Q.; Pan, J.; Liu, Y.; Si, H.; Lu, Z.; Han, X.; Gao, J.; Zuo, Z.; Zhang, H.; Jiang, S. Output energy enhancement in a mode-locked Er-doped fiber laser using CVD-Bi2Se3 as a saturable absorber. Opt. Express 2019, 27, 24670–24681.

52. Guo, Q.; Fan, X.; Gao, J.; Han, X.; Zhang, H.; Han, Y.; Jiang, S. Bi2Se3/mica optical modulator for high-energy mode-locked Er-doped fiber laser. Infrared Phys. Technol. 2020, 111, 103453.

53. Luo, Z.; Huang, Y.; Weng, J.; Cheng, H.; Lin, Z.; Xu, B.; Cai, Z.; Xu, H. 1.06 μm Q-switched ytterbium-doped fiber laser using few-layer topological insulator Bi2Se3 as a saturable absorber. Opt. Express 2013, 21, 29516–29522.

54. Li, P.; Zhang, G.; Zhang, H.; Zhao, C.; Chi, J.; Zhao, Z.; Yang, C.; Hu, H.; Yao, Y. Q-switched mode-locked Nd:YVO4 laser by topological insulator Bi2Te3 saturable absorber. IEEE Photonics Technol. Lett. 2014, 26, 1912–1915.

55. Chi, C.; Lee, J.; Koo, J.; Han Lee, J. All-normal-dispersion dissipative-soliton fiber laser at 1.06 μm using a bulk-structured Bi2Te3 topological insulator-deposited side-polished fiber. Laser Phys. 2014, 24, 105106.

56. Dou, Z.Y.; Song, Y.R.; Tian, J.R.; Liu, J.H.; Yu, Z.H.; Fang, X.H. Mode-locked ytterbium-doped fiber laser based on topological insulator: Bi2Se3. Opt. Express 2014, 22, 24055–24061.

57. Xu, B.; Wang, Y.; Peng, J.; Luo, Z.; Xu, H.; Cai, Z.; Weng, J. Topological insulator Bi2Se3 based Q-switched Nd:LiYF4 nanosecond laser at 1313 nm. Opt. Express 2015, 23, 7674–7680.

58. Xu, J.L.; Sun, Y.J.; He, J.L.; Wang, Y.; Zhu, Z.J.; You, Z.Y.; Li, J.F.; Chou, M.M.; Lee, C.K.; Tu, C.Y. Ultrasensitive nonlinear absorption response of large-size topological insulator and application in low-threshold bulk pulsed lasers. Sci. Rep. 2015, 5, 14856.

59. Wang, Y.R.; He, J.L.; Lee, C.K.; Sung, W.H.; Su, X.C.; Zhao, Y.; Zhang, B.T.; Wu, C.L.; He, G.B.; Lin, Y.Y.; et al. Ultralow saturation intensity topological insulator saturable absorber for gigahertz mode-locked solid-state lasers. IEEE Photonics J. 2018, 10, 1–10.

60. Luo, Z.; Liu, C.; Huang, Y.; Wu, D.; Wu, J.; Xu, H.; Cai, Z.; Lin, Z.; Sun, L.; Weng, J. Topological-insulator passively Q-switched double-clad fiber laser at 2 μm wavelength. IEEE J. Sel. Top. Quantum Electron. 2014, 20, 6739071.

61. Jung, M.; Lee, J.; Koo, J.; Park, J.; Song, Y.W.; Lee, K.; Lee, S.; Lee, J.H. A femtosecond pulse fiber laser at 1935 nm using a bulk-structured Bi2Te3 topological insulator. Opt. Express 2014, 22, 7865–7874.

62. Yin, K.; Zhang, B.; Li, L.; Jiang, T.; Zhou, X.; Hou, J. Soliton mode-locked fiber laser based on topological insulator Bi2Te3 nanosheets at 2 μm. Photonics Res. 2015, 3, 72–76.

63. Lee, J.; Ju, H.L. Femtosecond Tm–Ho co-doped fiber laser using a bulk-structured Bi2Se3 topological insulator. Chin. Phys. B 2018, 27, 152–159.

64. Loiko, P.; Bogusławski, J.; Serres, J.M.; Kifle, E.; Kowalczyk, M.; Mateos, X.; Sotor, J.; Zybała, R.; Mars, K.; MikuŁa, A.; et al. Sb2Te3 thin film for the passive Q-switching of a Tm:GdVO4 laser. Opt. Mater. Express 2018, 8, 1723.

65. Yin, K.; Jiang, T.; Zheng, X.; Yu, H.; Cheng, X.; Hou, J. Mid-infrared ultra-short mode-locked fiber laser utilizing topological insulator Bi2Te3 nano-sheets as the saturable absorber. arXiv 2015, arXiv:1505.06322.

66. Li, J.; Luo, H.; Wang, L.; Zhao, C.; Zhang, H.; Li, H.; Liu, Y. 3-μm Mid-infrared pulse generation using topological insulator as the saturable absorber. Opt. Lett. 2015, 40, 3659–3662.

67. Tang, P.; Wu, M.; Wang, Q.; Miao, L.; Huang, B.; Liu, J.; Zhao, C.; Wen, S. 2.8-μm pulsed Er3+: ZBLAN fiber laser modulated by topological insulator. IEEE Photonics Technol. Lett. 2016, 28, 1573–1576.

68. Li, W.; Wang, K.; Du, T.; Zou, J.; Li, Y.; Luo, Z. Miniaturized mid-Infrared all-fiber laser passively Q-switched by topological insulator Bi2Se3. In Proceedings of the 2018 Asia Communications and Photonics Conference (ACP), Hangzhou, China, 26–29 October 2018; pp. 1–3.

69. Chen, S.; Zhao, C.; Li, Y.; Huang, H.; Lu, S.; Zhang, H.; Wen, S. Broadband optical and microwave nonlinear response in topological insulator. Opt. Mater. Express 2014, 4, 587–596.

70. Lu, S.; Zhao, C.; Zou, Y.; Chen, S.; Chen, Y.; Li, Y.; Zhang, H.; Wen, S.; Tang, D. Third order nonlinear optical property of Bi2Se3. Opt. Express 2013, 21, 2072–2082.

71. Yu, H.; Zhang, H.; Wang, Y.; Zhao, C.; Wang, B.; Wen, S.; Zhang, H.; Wang, J. Topological insulator as an optical modulator for pulsed solid-state lasers. Laser Photonics Rev. 2013, 7, L77–L83.

72. Wu, D.; Cai, Z.; Zhong, Y.; Peng, J.; Weng, J.; Luo, Z.; Chen, N.; Xu, H. 635-nm visible Pr3+-doped ZBLAN fiber lasers Q-switched by topological insulators SAs. IEEE Photonics Technol. Lett. 2015, 27, 2379–2382.

73. Lin, H.Y.; Li, W.S.; Lan, J.L.; Guan, X.F.; Xu, H.Y.; Cai, Z.P. All-fiber passively Q-switched 604 nm praseodymium laser with a Bi2Se3 saturable absorber. Appl. Opt. 2017, 56, 802–805.

74. Chen, Y.; Jiang, G.; Chen, S.; Guo, Z.; Yu, X.; Zhao, C.; Zhang, H.; Bao, Q.; Wen, S.; Tang, D.; et al. Mechanically exfoliated black phosphorus as a new saturable absorber for both Q-switching and Mode-locking laser operation. Opt. Express 2015, 23, 12823–12833.

75. Glinka, Y.D.; Babakiray, S.; Johnson, T.A.; Bristow, A.D.; Holcomb, M.B.; Lederman, D. Ultrafast carrier dynamics in thin-films of the topological insulator Bi2Se3. Appl. Phys. Lett. 2013, 103, 151903.

76. Boguslawski, J.; Sotor, J.; Sobon, G.; Tarka, J.; Jagiello, J.; Macherzynski, W.; Lipinska, L.; Abramski, K.M. Mode-locked Er-doped fiber laser based on liquid phase exfoliated Sb2Te3 topological insulator. Laser Phys. 2014, 24, 105111.

77. Sotor, J.; Sobon, G.; Boguslawski, J.; Tarka, J.; Abramski, K. Sb2Te3 topological insulator based saturable absorber for Er-doped mode-locked fiber lasers. In Proceedings of the SPIE LASE, San Francisco, CA, USA, 9–12 February 2015; Volume 9344.

78. Wang, K.; Wang, J.; Fan, J.; Lotya, M.; O'Neill, A.; Fox, D.; Feng, Y.; Zhang, X.; Jiang, B.; Zhao, Q.; et al. Ultrafast saturable absorption of two-dimensional MoS2 nanosheets. ACS Nano 2013, 7, 9260–9267.

79. Zhang, H.; Lu, S.B.; Zheng, J.; Du, J.; Wen, S.C.; Tang, D.Y.; Loh, K.P. Molybdenum disulfide (MoS2) as a broadband saturable absorber for ultra-fast photonics. Opt. Express 2014, 22, 7249–7260.

80. Woodward, R.I.; Kelleher, E.J.R.; Runcorn, T.H.; Popov, S.V.; Torrisi, F.; Howe, R.C.T.; Hasan, T. Q-switched fiber laser with MoS2 saturable absorber. In Proceedings of the CLEO: Science and Innovations, Optical Society of America, San Jose, CA, USA, 8–13 June 2014; p. SM3H.6.

81. Xu, B.; Cheng, Y.; Wang, Y.; Huang, Y.; Peng, J.; Luo, Z.; Xu, H.; Cai, Z.; Weng, J.; Moncorge, R. Passively Q-switched Nd:YAlO3nanosecond laser using MoS2 as saturable absorber. Opt. Express 2014, 22, 28934–28940.

82. Zhao, G.; Han, S.; Wang, A.; Wu, Y.; Zhao, M.; Wang, Z.; Hao, X. "Chemical Weathering" exfoliation of atom-thick transition metal dichalcogenides and their ultrafast saturable absorption properties. Adv. Funct. Mater. 2015, 25, 5292–5299.

83. Hou, J.; Zhao, G.; Wu, Y.; He, J.; Hao, X. Femtosecond solid-state laser based on tungsten disulfide saturable absorber. Opt. Express 2015, 23, 27292–27298.

84. Lin, J.; Hu, Y.; Chen, C.; Gu, C.; Xu, L. Wavelength-tunable Yb-doped passively Q-switching fiber laser based on WS2 saturable absorber. Opt. Express 2015, 23, 29059–29064.

85. Cheng, C.; Liu, H.; Tan, Y.; Vazquez de Aldana, J.R.; Chen, F. Passively Q-switched waveguide lasers based on two-dimensional transition metal diselenide. Opt. Express 2016, 24, 10385–10390.

86. Wang, X.; Wang, Y.; Duan, L.; Li, L.; Sun, H. Passively Q-switched Nd:YAG laser via a WS2 saturable absorber. Opt. Commun. 2016, 367, 234–238.

87. Liu, H.; Luo, A.P.; Wang, F.Z.; Tang, R.; Liu, M.; Luo, Z.C.; Xu, W.C.; Zhao, C.J.; Zhang, H. Femtosecond pulse erbium-doped fiber laser by a few-layer MoS2 saturable absorber. Opt. Lett. 2014, 39, 4591–4594.

88. Liu, M.; Zheng, X.W.; Qi, Y.L.; Liu, H.; Luo, A.P.; Luo, Z.C.; Xu, W.C.; Zhao, C.J.; Zhang, H. Microfiber-based few-layer MoS2 saturable absorber for 2.5 GHz passively harmonic mode-locked fiber laser. Opt. Express 2014, 22, 22841–22846.

89. Huang, Y.; Luo, Z.; Li, Y.; Zhong, M.; Xu, B.; Che, K.; Xu, H.; Cai, Z.; Peng, J.; Weng, J. Widely-tunable, passively Q-switched erbium-doped fiber laser with few-layer MoS2 saturable absorber. Opt. Express 2014, 22, 25258–25266.

90. Khazaeizhad, R.; Kassani, S.H.; Jeong, H.; Yeom, D.I.; Oh, K. Mode-locking of Er-doped fiber laser using a multilayer MoS2 thin film as a saturable absorber in both anomalous and normal dispersion regimes. Opt. Express 2014, 22, 23732–23742.

91. Mao, D.; Wang, Y.; Ma, C.; Han, L.; Jiang, B.; Gan, X.; Hua, S.; Zhang, W.; Mei, T.; Zhao, J. WS2 mode-locked ultrafast fiber laser. Sci. Rep. 2015, 5, 7965.

92. Khazaeinezhad, R.; Kassani, S.H.; Hwanseong, J.; Kyung Jun, P.; Byoung Yoon, K.; Dong-Il, Y.; Kyunghwan, O. Ultrafast pulsed all-fiber laser based on tapered fiber enclosed by few-layer WS2 nanosheets. IEEE Photonics Technol. Lett. 2015, 27, 1581–1584.

93. Kassani, S.H.; Khazaeinezhad, R.; Jeong, H.; Nazari, T.; Yeom, D.I.; Oh, K. All-fiber Er-doped Q-Switched laser based on Tungsten Disulfide saturable absorber. Opt. Mater. Express 2015, 5, 373–379.

94. Ferrari, A.C.; Bonaccorso, F.; Fal'ko, V.; Novoselov, K.S.; Roche, S.; Boggild, P.; Borini, S.; Koppens, F.H.; Palermo, V.; Pugno, N.; et al. Science and technology roadmap for graphene, related two-dimensional crystals, and hybrid systems.

Nanoscale 2015, 7, 4598–4810.

95. Luo, Z.; Li, Y.; Zhong, M.; Huang, Y.; Wan, X.; Peng, J.; Weng, J. Nonlinear optical absorption of few-layer molybdenum diselenide (MoSe2) for passively mode-locked soliton fiber laser [Invited]. Photonics Res. 2015, 3, A79–A86.
96. Koo, J.; Park, J.; Lee, J.; Jhon, Y.M.; Lee, J.H. Femtosecond harmonic mode-locking of a fiber laser at 3.27 GHz using a bulk-like, MoSe2-based saturable absorber. Opt. Express 2016, 24, 10575–10589.
97. Liu, W.; Pang, L.; Han, H.; Liu, M.; Lei, M.; Fang, S.; Teng, H.; Wei, Z. Tungsten disulfide saturable absorbers for 67 fs mode-locked erbium-doped fiber lasers. Opt. Express 2017, 25, 2950–2959.
98. Liu, W.; Liu, M.; OuYang, Y.; Hou, H.; Lei, M.; Wei, Z. CVD-grown MoSe2 with high modulation depth for ultrafast mode-locked erbium-doped fiber laser. Nanotechnology 2018, 29, 394002.
99. Wang, S.; Yu, H.; Zhang, H.; Wang, A.; Zhao, M.; Chen, Y.; Mei, L.; Wang, J. Broadband few-layer MoS2 saturable absorbers. Adv. Mater. 2014, 26, 3538–3544.
100. Luo, Z.; Huang, Y.; Zhong, M.; Li, Y.; Wu, J.; Xu, B.; Xu, H.; Cai, Z.; Peng, J.; Weng, J. 1-, 1.5-, and 2-μm fiber lasers Q-switched by a broadband few-layer MoS2 saturable absorber. J. Light. Technol. 2014, 32, 4679–4686.
101. Kong, L.; Xie, G.; Yuan, P.; Qian, L.; Wang, S.; Yu, H.; Zhang, H. Passive Q-switching and Q-switched mode-locking operations of 2 μm Tm: CLNGG laser with MoS2 saturable absorber mirror. Photonics Res. 2015, 3, A47–A50.
102. Tian, Z.; Wu, K.; Kong, L.; Yang, N.; Wang, Y.; Chen, R.; Hu, W.; Xu, J.; Tang, Y. Mode-locked thulium fiber laser with MoS2. Laser Phys. Lett. 2015, 12, 065104.
103. Jung, M.; Lee, J.; Park, J.; Koo, J.; Jhon, Y.M.; Lee, J.H. Mode-locked, 1.94-μm, all-fiberized laser using WS2 based evanescent field interaction. Opt. Express 2015, 23, 19996–20006.
104. Lee, J.; Koo, J.; Lee, J.; Jhon, Y.M.; Lee, J.H. All-fiberized, femtosecond laser at 1912 nm using a bulk-like MoSe2 saturable absorber. Opt. Mater. Express 2017, 7, 2968–2979.
105. Wang, J.; Xu, Z.; Liu, W.; Yan, P.; Lu, W.; Li, J.; Chen, H.; Jiang, Z.; Wang, J.; Zhang, W.; et al. Ultrafast thulium-doped fiber laser mode locked by monolayer WSe2. IEEE J. Sel. Top. Quantum Electron. 2018, 24, 1–6.
106. Fan, M.; Li, T.; Zhao, S.; Li, G.; Ma, H.; Gao, X.; Krankel, C.; Huber, G. Watt-level passively Q-switched Er:Lu2O3 laser at 2.84 μm using MoS2. Opt. Lett. 2016, 41, 540–543.
107. Wei, C.; Luo, H.; Zhang, H.; Li, C.; Xie, J.; Li, J.; Liu, Y. Passively Q-switched mid-infrared fluoride fiber laser around 3 μm using a tungsten disulfide (WS2) saturable absorber. Laser Phys. Lett. 2016, 13, 105108.
108. Liu, X.; Zhang, S.; Yan, Z.; Guo, L.; Fan, X.; Lou, F.; Wang, M.; Gao, P.; Guo, G.; Li, T.; et al. WSe2 as a saturable absorber for a passively Q-switched Ho,Pr:LLF laser at 295 μm. Opt. Mater. Express 2018, 8, 1213.
109. Zhang, S.; Liu, X.; Guo, L.; Fan, M.; Lou, F.; Gao, P.; Guo, G.; Yang, J.; Liu, J.; Li, T.; et al. Passively Q-switched Ho,Pr:LLF bulk slab laser at 2.95μm based on MoS2 saturable absorber. IEEE Photonics Technol. Lett. 2017, 29, 2258–2261.
110. Guo, C.; Wei, J.; Yan, P.; Luo, R.; Ruan, S.; Wang, J.; Guo, B.; Hua, P.; Lue, Q. Mode-locked fiber laser at 2.8 μm using a chemical-vapor-deposited WSe2 saturable absorber mirror. Appl. Phys. Express 2020, 13, 012013.
111. Chen, B.; Zhang, X.; Wu, K.; Wang, H.; Wang, J.; Chen, J. Q-switched fiber laser based on transition metal dichalcogenides MoS2, MoSe2, WS2, and WSe2. Opt. Express 2015, 23, 26723–26737.
112. Du, J.; Wang, Q.; Jiang, G.; Xu, C.; Zhao, C.; Xiang, Y.; Chen, Y.; Wen, S.; Zhang, H. Ytterbium-doped fiber laser passively mode locked by few-layer Molybdenum Disulfide (MoS2) saturable absorber functioned with evanescent field interaction. Sci. Rep. 2014, 4, 6346.
113. Liu, S.; Lv, R.; Wang, Y.; Wang, J.; Wang, Y.; Wang, H. Passively mode-locked fiber laser with WS2/SiO2 saturable absorber fabricated by Sol-Gel technique. ACS Appl. Mater. Interfaces 2020, 12, 29625–29630.
114. Cheng, C.; Li, Z.; Dong, N.; Wang, J.; Chen, F. Tin diselenide as a new saturable absorber for generation of laser pulses at 1 μm. Opt. Express 2017, 25, 6132–6140.
115. Li, J.; Zhao, Y.; Chen, Q.; Niu, K.; Sun, R.; Zhang, H. Passively mode-locked ytterbium-doped fiber laser based on SnS2 as saturable absorber. IEEE Photonics J. 2017, 9, 1–7.
116. Niu, K.; Chen, Q.; Sun, R.; Man, B.; Zhang, H. Passively Q-switched erbium-doped fiber laser based on SnS2 saturable absorber. Opt. Mater. Express 2017, 7, 3934–3943.
117. Niu, K.; Sun, R.; Chen, Q.; Man, B.; Zhang, H. Passively mode-locked Er-doped fiber laser based on SnS2 nanosheets as a saturable absorber. Photonics Res. 2018, 6, 72–76.
118. Yao, Y.; Zhang, F.; Chen, B.; Zhao, Y.; Cui, N.; Sun, D.; Liu, S.; Zhang, Y.; Zhang, H.; Zhang, H. Nonlinear optical property and mid-infrared Q-switched laser application at 2.8 μm of PtSe2 material. Opt. Laser Technol. 2021, 139, 106983.

119. Li, D.; Jussila, H.; Karvonen, L.; Ye, G.; Lipsanen, H.; Chen, X.; Sun, Z. Polarization and thickness dependent absorption properties of black phosphorus: New saturable absorber for ultrafast pulse generation. Sci. Rep. 2015, 5, 15899.

120. Chen, Y.; Chen, S.; Liu, J.; Gao, Y.; Zhang, W. Sub-300 femtosecond soliton tunable fiber laser with all-anomalous dispersion passively mode locked by black phosphorus. Opt. Express 2016, 24, 13316–13324.

121. Song, Y.; Chen, S.; Zhang, Q.; Li, L.; Zhao, L.; Zhang, H.; Tang, D. Vector soliton fiber laser passively mode locked by few layer black phosphorus-based optical saturable absorber. Opt. Express 2016, 24, 25933–25942.

122. Yun, L. Black phosphorus saturable absorber for dual-wavelength polarization-locked vector soliton generation. Opt. Express 2017, 25, 32380–32385.

123. Jin, X.; Hu, G.; Zhang, M.; Hu, Y.; Albrow-Owen, T.; Howe, R.C.T.; Wu, T.C.; Wu, Q.; Zheng, Z.; Hasan, T. 102 fs pulse generation from a long-term stable, inkjet-printed black phosphorus-mode-locked fiber laser. Opt. Express 2018, 26, 12506–12513.

124. Zhang, B.; Lou, F.; Zhao, R.; He, J.; Li, J.; Su, X.; Ning, J.; Yang, K. Exfoliated layers of black phosphorus as saturable absorber for ultrafast solid-state laser. Opt. Lett. 2015, 40, 3691–3694.

125. Ma, J.; Lu, S.; Guo, Z.; Xu, X.; Zhang, H.; Tang, D.; Fan, D. Few-layer black phosphorus based saturable absorber mirror for pulsed solid-state lasers. Opt. Express 2015, 23, 22643–22648.

126. Al-Masoodi, A.H.H.; Ahmed, M.H.M.; Latiff, A.A.; Arof, H.; Harun, S.W. Q-switched ytterbium-doped fiber laser using black phosphorus as saturable absorber. Chin. Phys. Lett. 2016, 33, 054206.

127. Su, X.; Wang, Y.; Zhang, B.; Zhao, R.; Yang, K.; He, J.; Hu, Q.; Jia, Z.; Tao, X. Femtosecond solid-state laser based on a few-layered black phosphorus saturable absorber. Opt. Lett. 2016, 41, 1945–1948.

128. Rashid, F.A.A.; Azzuhri, S.R.; Salim, M.A.M.; Shaharuddin, R.A.; Ismail, M.A.; Ismail, M.F.; Razak, M.Z.A.; Ahmad, H. Using a black phosphorus saturable absorber to generate dual wavelengths in a Q-switched ytterbium-doped fiber laser. Laser Phys. Lett. 2016, 13, 085102.

129. Ahmad, H.; Salim, M.A.M.; Thambiratnam, K.; Norizan, S.F.; Harun, S.W. A black phosphorus-based tunable Q-switched ytterbium fiber laser. Laser Phys. Lett. 2016, 13, 095103.

130. Huang, K.X.; Lu, B.L.; Li, D.; Qi, X.Y.; Chen, H.W.; Wang, N.; Wen, Z.R.; Bai, J.T. Black phosphorus flakes covered microfiber for Q-switched ytterbium-doped fiber laser. Appl. Opt. 2017, 56, 6427–6431.

131. Wang, D.; Song, H.; Long, X.; Li, L. Switchable and tunable multi-wavelength emissions in pulsed ytterbium fiber lasers with black phosphorus saturable absorbers and polarization-maintaining fiber Bragg gratings. Opt. Commun. 2019, 452, 373–379.

132. Sotor, J.; Sobon, G.; Kowalczyk, M.; Macherzynski, W.; Paletko, P.; Abramski, K.M. Ultrafast thulium-doped fiber laser mode locked with black phosphorus. Opt. Lett. 2015, 40, 3885–3888.

133. Yu, H.; Zheng, X.; Yin, K.; Cheng, X.; Jiang, T. Nanosecond passively Q-switched thulium/holmium-doped fiber laser based on black phosphorus nanoplatelets. Opt. Mater. Express 2016, 6, 603–609.

134. Chu, Z.Z.; Liu, J.; Guo, Z.N.; Zhang, H. 2 μm passively Q-switched laser based on black phosphorus. Opt. Mater. Express 2016, 6, 2374–2379.

135. Zhang, H.; He, J.; Wang, Z.; Hou, J.; Zhang, B.; Zhao, R.; Han, K.; Yang, K.; Nie, H.; Sun, X. Dual-wavelength, passively Q-switched Tm:YAP laser with black phosphorus saturable absorber. Opt. Mater. Express 2016, 6, 2328–2335.

136. Pawliszewska, M.; Ge, Y.; Li, Z.; Zhang, H.; Sotor, J. Fundamental and harmonic mode-locking at 2.1 μm with black phosphorus saturable absorber. Opt. Express 2017, 25, 16916–16921.

137. Qin, Z.; Xie, G.; Zhang, H.; Zhao, C.; Yuan, P.; Wen, S.; Qian, L. Black phosphorus as saturable absorber for the Q-switched Er:ZBLAN fiber laser at 2.8 μm. Opt. Express 2015, 23, 24713–24718.

138. Qin, Z.; Xie, G.; Zhao, C.; Wen, S.; Yuan, P.; Qian, L. Mid-infrared mode-locked pulse generation with multilayer black phosphorus as saturable absorber. Opt. Lett. 2016, 41, 56–59.

139. Kong, L.; Qin, Z.; Xie, G.; Guo, Z.; Zhang, H.; Yuan, P.; Qian, L. Black phosphorus as broadband saturable absorber for pulsed lasers from 1 μm to 2.7 μm wavelength. Laser Phys. Lett. 2016, 13, 045801.

140. Li, J.F.; Luo, H.Y.; Zhai, B.; Lu, R.G.; Guo, Z.N.; Zhang, H.; Liu, Y. Black phosphorus: A two-dimension saturable absorption material for mid-infrared Q-switched and mode-locked fiber lasers. Sci. Rep. 2016, 6, 30361.

141. Liu, J.; Liu, J.; Guo, Z.; Zhang, H.; Ma, W.; Wang, J.; Su, L. Dual-wavelength Q-switched Er:SrF2 laser with a black phosphorus absorber in the mid-infrared region. Opt. Express 2016, 24, 30289–30295.

142. Woodward, R.I.; Majewski, M.R.; Macadam, N.; Hu, G.; Albrow-Owen, T.; Hasan, T.; Jackson, S.D. Q-switched Dy:ZBLAN fiber lasers beyond 3 μm: Comparison of pulse generation using acousto-optic modulation and inkjet-printed black

phosphorus. Opt. Express 2019, 27, 15032–15045.

143. Guo, Z.; Zhang, H.; Lu, S.; Wang, Z.; Tang, S.; Shao, J.; Sun, Z.; Xie, H.; Wang, H.; Yu, X.F.; et al. From black phosphorus to phosphorene: Basic solvent exfoliation, evolution of raman scattering, and applications to ultrafast photonics. Adv. Funct. Mater. 2015, 25, 6996–7002.
144. Morita, A. Semiconducting black phosphorus. Appl. Phys. A 1986, 39, 227–242.
145. Tran, V.; Soklaski, R.; Liang, Y.; Yang, L. Layer-controlled band gap and anisotropic excitons in few-layer black phosphorus. Phys. Rev. B 2014, 89, 235319.
146. Island, J.O.; Steele, G.A.; van der Zant, H.S.; Castellanos-Gomez, A. Environmental instability of few-layer black phosphorus. 2D Mater. 2015, 2, 011002.
147. Wang, X.; Jones, A.M.; Seyler, K.L.; Tran, V.; Jia, Y.; Zhao, H.; Wang, H.; Yang, L.; Xu, X.; Xia, F. Highly anisotropic and robust excitons in monolayer black phosphorus. Nat. Nanotechnol. 2015, 10, 517–521.
148. Castellanos-Gomez, A.; Vicarelli, L.; Prada, E.; Island, J.O.; Narasimha-Acharya, K.; Blanter, S.I.; Groenendijk, D.J.; Buscema, M.; Steele, G.A.; Alvarez, J. Isolation and characterization of few-layer black phosphorus. 2D Mater. 2014, 1, 025001.
149. Mikulla, B.; Leng, L.; Sears, S.; Collings, B.C.; Arend, M.; Bergman, K. Broad-band high-repetition-rate source for spectrally sliced WDM. IEEE Photonics Technol. Lett. 1999, 11, 418–420.
150. Ma, C.; Wang, C.; Gao, B.; Adams, J.; Wu, G.; Zhang, H. Recent progress in ultrafast lasers based on 2D materials as a saturable absorber. Appl. Phys. Rev. 2019, 6, 041304.
151. McFerran, J.J. Échelle spectrograph calibration with a frequency comb based on a harmonically mode-locked fiber laser: A proposal. Appl. Opt. 2009, 48, 2752–2759.